Entanglement Effects in Semiflexible Polymer Solutions. 1. Zero-Shear Viscosity of Poly(*n*-hexyl isocyanate) Solutions

Atsuyuki Ohshima, Hiroyuki Kudo, Takahiro Sato,* and Akio Teramoto

Department of Macromolecular Science, Osaka University, Toyonaka, Osaka 560, Japan

Received March 14, 1995; Revised Manuscript Received June 20, 1995[⊗]

ABSTRACT: Zero-shear viscosities η_0 of dichloromethane solutions of a semiflexible polymer, poly(*n*-hexyl isocyanate) (PHIC), were measured over a wide concentration range covering from dilute to concentrated isotropic regimes. Eight different molecular weight PHIC samples used for viscometry had the Kuhn statistical segment numbers N ranging from 0.80 to 97. The solution viscosity behavior of PHIC with $N \lesssim 10$ resembled that of rigid polymers [e.g., poly(γ-benzyl L-glutamate), schizophyllan, and xanthan], while η_0 for PHIC solutions with larger N almost obeyed the following power law at high concentration ranges: $\eta_0 \propto c^{3.6}M^4$ (c, polymer mass concentration; M, molecular weight). The power law behavior of η_0 is characteristic of flexible polymer solutions, although the exponents for the PHIC solutions are different from those of flexible polymer solutions. The viscosity results of PHIC solutions were compared with the fuzzy cylinder model theory recently proposed. Agreements between theory and experiment were found for PHIC solutions with $N \lesssim 8$, but not for PHIC solutions with $N \geq 15$. From this result, it was concluded that the validity of the fuzzy cylinder model theory is limited to polymer chains with N smaller than ca. 10. No suitable theory was found for PHIC solutions with $N \geq 15$.

1. Introduction

Entanglement effects on polymer dynamics strongly depend on the polymer chain stiffness. For example, zero-shear viscosities η_0 of stiff polymer solutions exhibit remarkably different polymer molecular weight and concentration dependences from those of flexible polymer solutions.[1-4] In their monograph,[5] Doi and Edwards discussed entanglement effects for two extremes, the random coil and the rigid rod, by using the tube model. However, their model cannot be applied to semiflexible polymer systems as it stands.

Odijk,[6] Doi,[7] and Semenov[8] independently extended Doi-Edwards' theory to semiflexible polymer systems. The reptation model they used assumes that the internal motion lateral to the semiflexible chain contour is prohibited by entanglements during the time scale of global chain motions, i.e., the end-over-end rotation and the center-of-mass translation of the chain. This assumption might be valid for considerably flexible polymer chains in highly concentrated solutions, but experimental data for stiff or semiflexible polymer systems have not supported the reptation model theories yet.[7]

Recently, Sato et al.[9] treated the entanglement effect of semiflexible polymer chains on the basis of a cylindrical smoothed density model referred to as the "fuzzy cylinder". The basic assumption of their theory is that local conformational changes of semiflexible chains are much faster than global motions of the chain in concentrated solution, which may be relevant to polymers with high stiffness. On this assumption, one can identify the semiflexible chain with the fuzzy cylinder, in a discussion of global chain motions in solution.

Previous studies[9-12] demonstrated favorable comparisons of the fuzzy cylinder model theory with experimental results of zero-shear viscosities for several stiff-chain polymer solutions as well as of rotational and translational self-diffusion coefficients for some stiff polymers in moderately concentrated solutions. These results justify the assumption of the fast local chain motion compared with the slow global chain motion in the theory.

However, the previous comparison with the fuzzy cylinder model theory was limited to experimental data for polymer samples with Kuhn's statistical segment numbers N smaller than ca. 10. Since flexible polymer chains usually have N larger than a few hundred, polymer chains with $N \sim 10$ are still considerably stiff.

The present study was undertaken to explore the limit of the validity of the fuzzy cylinder model by comparing the theory with experiment. A semiflexible polymer, poly(*n*-hexyl isocyanate) (PHIC) was chosen for this purpose. This polymer has the persistence length q of 21 nm in dichloromethane (DCM) at 20 °C[13,14] and is much more flexible than the polymers tested in the previous studies: schizophyllan (q = 200 nm), poly(γ-benzyl L-glutamate) (q = 150 nm), and xanthan (q = 120 nm). PHIC has the following characteristics: (1) this polymer can be effectively fractionated to obtain narrow molecular-weight-distribution samples;[13,15] (2) it has good solubility to DCM, toluene, etc.;[14,16,17] (3) it is well characterized molecularly from dilute solution studies.[13-15,18] Owing to these characteristics, PHIC is a suitable semiflexible polymer for testing the validity of the fuzzy cylinder model theory.

The viscosity behavior of polyisocyanate solutions was studied previously by Aharoni[19-21] and Aharoni and Walsh.[22,23] However, they used unfractionated polyisocyanate samples with considerably wide molecular weight distributions and measured the solution viscosity at a high shear rate. Therefore, their viscosity data are not suitable for the present purpose.

In the present study, we measured zero-shear viscosities for isotropic DCM solutions of fractionated PHIC samples with a wide range of the PHIC concentration and molecular weight and compared them with the fuzzy cylinder model theory previously formulated. The Kuhn segment numbers N of the PHIC samples used range from 0.80 to 97. This largest number is comparable to N of the usual flexible polymers with normal molecular weights.

2. Experimental Section

2.1. Samples. Poly(*n*-hexyl isocyanate) (PHIC) samples were prepared by polymerization of *n*-hexyl isocyanate (Kanto Chemical Co., Ltd.)[13] followed by fractionation with benzene

[⊗] Abstract published in *Advance ACS Abstracts,* August 1, 1995.

0024-9297/95/2228-6095$09.00/0

Table 1. PHIC Samples Used for Viscometry

sample	$M/10^4$	N^d	$[\eta]/10^2$ cm^3 g^{-1} ^{e}	M_w/M_n	c_I/g cm^{-3} ^{f}
P-2	2.5[b]	0.80	0.407	1.02	0.30
O-2	3.5[a]	1.1	0.724	1.02	0.28
N-2	6.7[a]	2.2	1.60	1.02	0.25
M-2	13.5[a]	4.3	3.20	1.04	0.24
I-2	25[a]	8.0	5.97	1.10	
J-2	48[a]	15	10.2		
G-2	110[c]	35	19.5		
H-1-2	300[c]	97	42.7		

[a] M_w determined by light scattering. [b] M_v estimated from $[\eta]$ in 20 °C DCM with the $[\eta]-M_w$ relation obtained by Itou et al.[13] and Jinbo et al.[14] [c] M_v estimated from $[\eta]$ in 25 °C *n*-hexane with the $[\eta]-M_w$ relation obtained by Murakami et al.[15] [d] Kuhn segment number in 20 °C DCM estimated from M with the wormlike chain parameters q = 21 nm and M_L (the molar mass per unit contour length) = 740 nm^{-1}.[13,14] [e] Intrinsic viscosity in 20 °C DCM. [f] Phase boundary concentration between the isotropic phase and isotropic–nematic biphasic regions for the DCM solution estimated by the interpolation of Itou and Teramoto's data.[16]

and methanol as solvent and precipitant, respectively.[14] Eight fractionated PHIC samples were chosen for the viscosity experiment. The molecular characteristics of these samples are listed in Table 1. For four samples, the weight-average molecular weight (M_w) was determined by light scattering; its procedure is described elsewhere.[14] The intrinsic viscosity ($[\eta]$)–M_w relation for the four PHIC samples in 20 °C DCM (cf. the second and fourth columns in Table 1) agreed with the same relation previously obtained.[13,14] For the other four samples, the viscosity-average molecular weight (M_v) was estimated from $[\eta]$ in 20 °C DCM or in 25 °C *n*-hexane by using the previous $[\eta]-M_w$ relation. In the following, M_v is not differentiated from M_w and both are denoted by M. The ratios of the weight-average to number-average molecular weights (M_w/M_n) determined from GPC ranged from 1.02 to 1.10 for the PHIC samples examined.

2.2. Viscometry. Shear viscosities of PHIC solutions above 0.2 Pa s were measured as a function of the shear rate by a magnetically controlled ball rheometer[4,24] with a 0.5-mm-radius steel ball. Test solutions with high viscosities were prepared (or diluted) in a test tube with the inner diameter of 10 mm illustrated in Figure 1. When DCM was poured into the test tube with a high molecular weight PHIC sample (or a concentrated viscous PHIC solution), the homogenization of the mixture was usually difficult in the test tube especially containing a long mixture column. The following procedure was used for the homogenization. First, the tubing (a) in Figure 1 was inserted into the bottom of the test tube and sucked a bottom part of the mixture (b). Then it was pull up to the meniscus of the mixture, and the solution in the tubing was squeezed out. This operation was repeated many times until the upper and bottom parts of the mixture were homogenized. Then, the tubing (a) was pulled up from the test solution (b) and fixed by screwing on the stopper (e), and the test tube (c) was directly set on the ball rheometer to measure the viscosity. Since DCM is a volatile solvent, the polymer concentration of the test solution was estimated from the weight of the solution measured just before each viscosity measurement. Shear viscosities of less viscous solutions were measured by four-bulb capillary-type low shear viscometers.

Viscosity measurements were made at 20 °C. The shear rate dependence of PHIC solutions was so weak that the extrapolation of shear viscosities to zero shear rate was easily performed to obtain the zero-shear viscosity.

3. Results

Figure 2 shows the double-logarithmic plot of the zero-shear viscosity (η_0) vs the polymer mass concentration (c) for DCM solutions of eight PHIC samples at 20 °C. Except for two high molecular weight samples, the data points for each sample follow a curve concave upward in the c range examined. On the other hand, almost straight lines are seen for the data points for the two

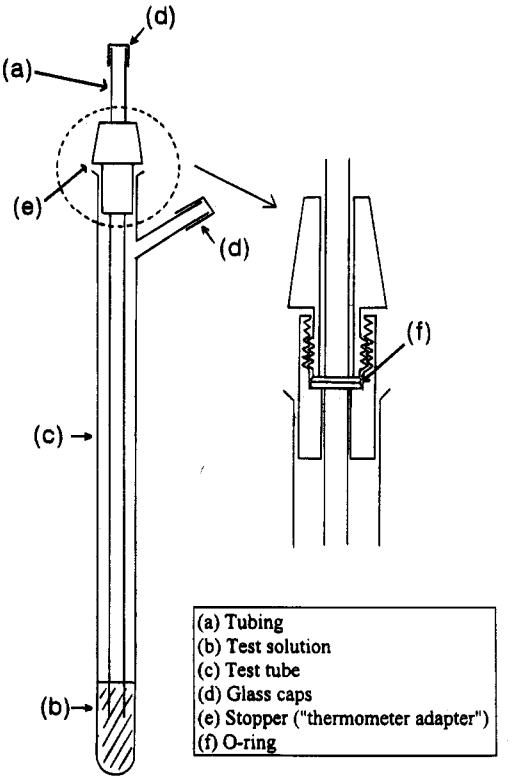

Figure 1. Schematic diagram of the test tube used for viscometry by the ball rheometer.

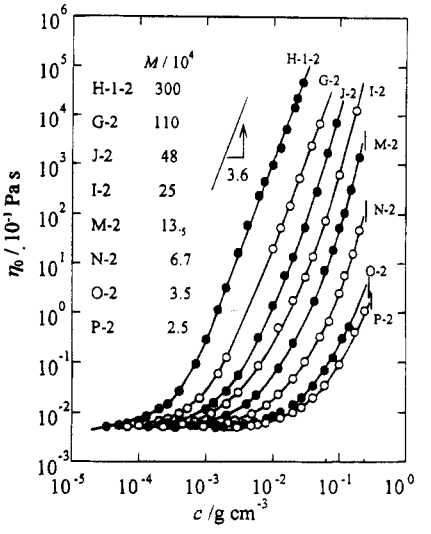

Figure 2. Polymer concentration dependence of the zero-shear viscosity η_0 for DCM solutions of eight PHIC samples at 20 °C. The vertical segments in the figure indicate the phase boundary concentrations c_I between the isotropic phase and biphasic regions for the four lowest molecular weight samples.

highest molecular weight samples, with the slope of 3.6 at $c \gtrsim 0.002$ g/cm^3 (sample G-2) and at $c \gtrsim 0.0007$ g/cm^3 (sample H-1-2). The former concentration dependence is similar to those observed in solutions of rigid polymers of schizophyllan[2,3] and xanthan,[4] while the latter power law dependence is often reported for semidilute solutions of flexible polymers.[5,25,26]

Figure 3 shows the molecular weight dependence of η_0 for PHIC solutions at fixed c. The data points at each fixed c follow a curve concave upward, and the slope of each curve is ca. 4 at a high M region. This exponent 4 is much smaller than the corresponding exponent for concentrated isotropic solutions of more rigid polymers,

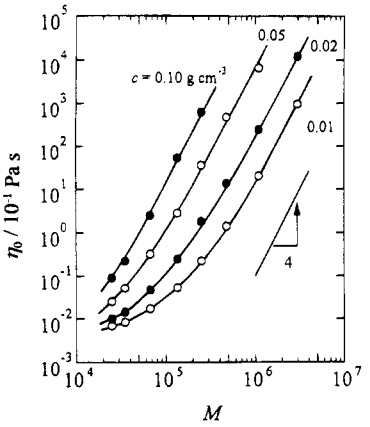

Figure 3. Molecular weight dependence of η_0 for DCM solutions of PHIC at different polymer mass concentrations.

schizophyllan[3] and xanthan[4] (5–7), but slightly larger than that for concentrated solutions of entangled flexible polymers[5,25,27] (3.4).

On the basis of the dynamic scaling hypothesis, η_0 for semidilute solutions of flexible polymers is often expressed in the scaling functional form: $\eta_0 = \eta^{(S)}F(c/c^*)$.[5,28] Here, $\eta^{(S)}$ is the solvent viscosity, $F(x)$ is a scaling function, and c^* is the overlap concentration usually defined by

$$c^* = 3M_w/4\pi\langle S^2\rangle^{3/2} \quad \text{or} \quad 1/[\eta] \tag{1}$$

Using the latter definition of c^*, i.e., $c^* = 1/[\eta]$, we plot $\eta_r \equiv \eta_0/\eta^{(S)}$ against $c[\eta]$ in Figure 4. The data points for different molecular weight samples do not form a composite curve. The use of the former definition of c^* in eq 1 did not improve the scattering of the data points. A similar scattering plot of η_r vs $c[\eta]$ was obtained also for aqueous solutions of xanthan in a previous study.[4] These results indicate that the dynamical scaling with eq 1 does not hold for semiflexible polymer solution systems. It may be worth noting that the osmotic compressibility of moderately concentrated solutions of PHIC dissolved in DCM was not a scaling function of c/c^* either, when c^* was equated to $1/A_2M$ (A_2, the second virial coefficient).[14]

4. Discussion

4.1. Fuzzy Cylinder Model Theory.[9,12] As mentioned in the Introduction, the theory is based on the fact that local conformational changes of semiflexible chains are much faster than global motions (the end-over-end rotation and the center-of-mass translation) of the chain in a concentrated solution. The fast local conformational changes distribute segments of the chain around the chain end-to-end axis, and each chain may be identified by a cylindrical smoothed density model (the fuzzy cylinder model). The average length (L_e) and the average diameter (d_e) of the fuzzy cylinder are defined as

$$L_e = \langle R^2\rangle^{1/2}, \qquad d_e = (\langle H^2\rangle + d^2)^{1/2} \tag{2}$$

where $\langle R^2\rangle$, $\langle H^2\rangle$, and d are respectively the mean-square end-to-end distance, the mean-square distance between the chain midpoint and the end-to-end axis, and the diameter of the chain. The first two quantities can be calculated from N and q.[9]

We express the zero-shear viscosity η_0 of an isotropic solution containing these fuzzy cylinders by

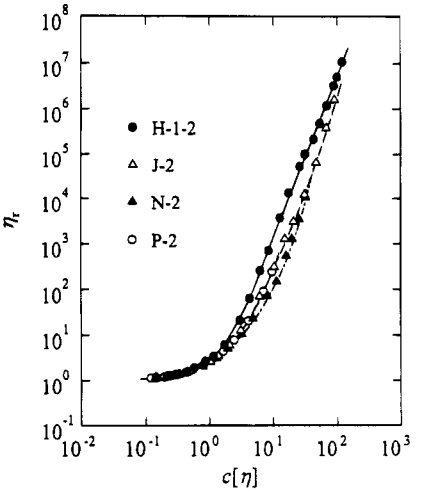

Figure 4. Plot of the relative viscosity (η_r) vs the reduced polymer concentration ($c[\eta]$) for solutions of four PHIC samples in DCM.

$$\eta_0 = \eta^{(S)}\left\{1 + [\eta]c\left[1 + \frac{3}{4}\gamma\chi^2\left(\frac{D_{r0}}{D_r} - 1\right)\right]\right\} \tag{3}$$

where $\eta^{(S)}$ is the solvent viscosity, $[\eta]$ is the polymer intrinsic viscosity, D_r and D_{r0} are the rotational diffusion coefficients at the polymer mass concentration c and at infinite dilution, respectively, and γ and χ are hydrodynamic factors which can be calculated from the axial ratio of the chain (see ref 9). It should be noted that eq 3 does not include the effect of the intermolecular hydrodynamic interaction, which may be minor in η_0 of highly entangled systems.

The entanglement effect on the rotational diffusion of the chain was treated by a mean-field Green function method for the fuzzy cylinder model. The formulated D_r/D_{r0} is written as

$$D_r/D_{r0} = [1 + 1350^{-1/2}(L_e^4/L)c'X'(D_{||0}/D_{||})^{1/2}]^{-2} \tag{4}$$

Here L is the chain contour length, c' is the polymer number concentration ($=cN_A/M$; N_A, Avogadro's constant), and $D_{||}$ and $D_{||0}$ are the longitudinal diffusion coefficients of the chain at concentration c and at infinite dilution, respectively. The longitudinal diffusion of the chain affects the lifetime of the entanglement between fuzzy cylinders. The numerical constant 1350 in the above equation was estimated by Teraoka et al.[29] from the calculations of stochastic geometry and probability of the entanglement for infinitely thin rods with the cage model.

The quantity X' in eq 4 is given by

$$X' \equiv f_r(d_e/L_e)(F_{||0}/F_{r0})^{1/2} \tag{5}$$

where $F_{||0}$ and F_{r0} are respectively correction factors for $D_{||0}$ and D_{r0} considering the flexibility and finite thickness of the chain, both of which can be calculated from N and the axial ratio of the chain,[9] and the function $f_r(d_e/L_e)$ takes into account an effect of segment fluctuation inside the fuzzy cylinder on the entanglement, given by

$$f_r(x) = (1 + C_r x)^3\left(1 - \frac{1}{5}C_r x\right) \tag{6}$$

The parameter C_r measures this fluctuation effect, and the empirical expression

$$C_r = \frac{1}{2}\{\tanh[(N - N^*)/\Delta] + 1\} \quad (7)$$

was proposed from the previous comparison of the fuzzy cylinder model theory with η_0 data of aqueous schizophyllan and xanthan.[12] Here, N^* and Δ are numerical constants. The factor $f_r(d_e/L_e)$ changes from 1 to 2.56 for probable values of d_e/L_e and C_r, and then its approximate value (and also of X') is sufficient for eq 4.

The ratio $D_{\parallel 0}/D_{\parallel}$ in eq 4 was formulated by the hole theory. Assuming that the longitudinal diffusion of a chain needs a free space (occupied by no neighboring chain segments) larger than a "critical hole" in front of the chain, the hole theory gives

$$D_{\parallel 0}/D_{\parallel} = \exp(V_{ex}^* c') \quad (8)$$

where V_{ex}^* is the excluded volume between the critical hole and a neighboring polymer chain. The critical hole was assumed to be similar in shape to the fuzzy cylinder representing the diffusing chain with the similitude ratio λ^*, and V_{ex}^* was expressed in terms of molecular parameters and λ^* (see eq 17 in ref 9).

4.2. Comparison between Theory and Experiment. To calculate η_0 for isotropic solutions of PHIC by eqs 3–8, we need the following parameters in the equations.

(1) The molecular parameters L_e, d_e, L, and N. They are estimated from M by eq 2 with $M_L = 740$ nm^{-1}, $q = 21$ nm, and $d = 1.6$ nm (cf. Table 1). These wormlike cylinder parameters were obtained from dilute solution studies of Itou et al.[13] and Jinbo et al.[14]

(2) The hydrodynamic parameters γ, χ, $F_{\parallel 0}$, and F_{r0}. These parameters are calculated from L/d and N.

(3) $\eta^{(S)}$ and $[\eta]$. The experimental values are used for them.

(4) The parameters N^* and Δ (in C_r) and λ^* (in V_{ex}^*). They are taken as adjustable parameters.

If we choose $N^* = \Delta = 4$ and $\lambda^* = 0.06$, the theoretical curves calculated by eqs 3–8 satisfactorily fit the experimental data points for the five lowest molecular weight PHIC samples as shown in Figure 5a. This good fitting verifies the validity of the fuzzy cylinder model for the semiflexible polymer PHIC with $N \leq 8$. The value of λ^* chosen for PHIC ($q = 21$ nm) in DCM is smaller than those for stiffer polymers, i.e., $\lambda^* = 0.13$ for schizophyllan ($q = 200$ nm) and $\lambda^* = 0.11$ for xanthan ($q = 120$ nm), which were determined in a previous study.[9] This indicates that the jamming effect on the longitudinal diffusion for PHIC is less effective than that for the stiffer polysaccharides, although we cannot explain the reason for this result. The values of N^* and Δ chosen for PHIC are essentially the same as those determined for the stiffer polysaccharides[12] ($N^* = 6$ and $\Delta = 4$).

Figure 5b compares the theoretical values calculated by eqs 3–8 with the same λ^*, N^*, and Δ with the experimental data for the three highest molecular weight PHIC samples with $N \geq 15$. For sample J-2 with $N = 15$, the data points deviate upward from the theoretical curves at an intermediate c region. For the higher molecular weight samples G-2 and H-1-2, the deviations are more enhanced than those for sample J-2, although the experimental values tend to approach the theoretical ones again at higher concentrations. From these results, it is concluded that the fuzzy cylinder model theory as it stands is not accurate for PHIC with N larger than 15.

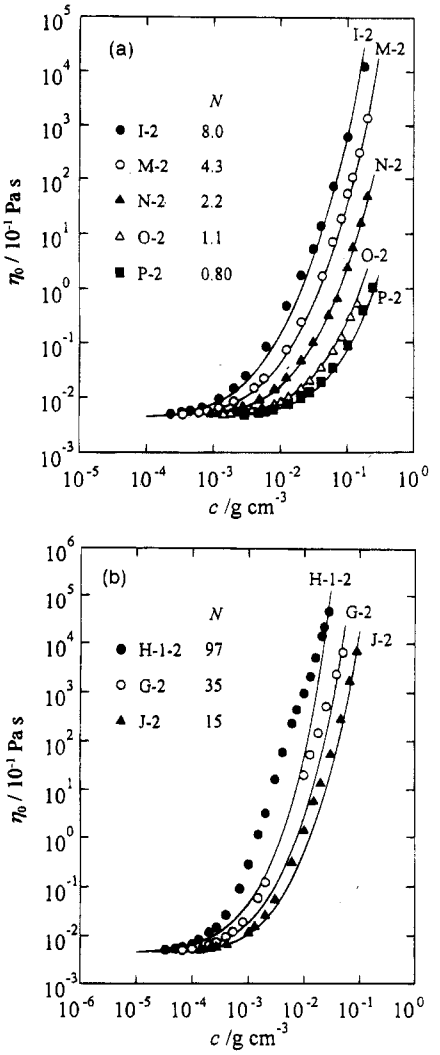

Figure 5. Comparison of η_0 of PHIC solutions with the fuzzy cylinder model theory: (a) PHIC samples with N from 0.80 to 8.0; (b) PHIC samples with N from 15 to 97; circles, experimental data; curves, theoretical values calculated by eqs 3–8 with $\lambda^* = 0.06$ and $N^* = \Delta = 4$ (see text).

The reptation theories of Odijk[6] and Doi[7] predict that when L of the semiflexible polymer exceeds q, the rotational relaxation time for a semiflexible polymer becomes identical with that for flexible polymers. This prediction leads one to the M^3 dependence of η_0[5] for semiflexible polymers with $N \gtrsim 1$. However, η_0 of PHIC solutions is approximately proportional to M^4 at high M regions (cf. Figure 3), and it is difficult to explain the viscosity behavior of high molecular weight PHIC solutions by the reptation theories. One may notice in Figure 2 that the exponent 3.6 of the c dependence of η_0 for high molecular weight PHIC solutions would be consistent with the prediction (3.75)[5,28] by the reptation theory combined with a scaling argument for flexible polymer–good solvent systems. However, this does not validate the scaling argument, because the prediction is based on the M^3 dependence of η_0 which is inconsistent with the experiment. At present, we have no suitable model which explains the viscosity behavior of PHIC solutions with $N \geq 15$.

5. Conclusions

The present study has compared zero-shear viscosities (η_0) of isotropic solutions of a semiflexible polymer, PHIC, with the fuzzy cylinder model theory. Agree-

ments between theory and experiment have been obtained for PHIC solutions with $N \leq 8$ but not for PHIC solutions with $N \geq 15$. The former agreements confirm the conclusion of the previous studies[9,12] that the fuzzy cylinder model theory is accurate to describe the global dynamics of stiff polymers (schizophyllan and xanthan) with $N \lesssim 10$. On the other hand, the latter disagreements imply inaccuracy of the fuzzy cylinder model theory for such semiflexible chains. However, the viscosity behavior of the high molecular weight PHIC solutions cannot be explained by other theories available at present, including reptation theories for semiflexible polymers.[6-8]

Acknowledgment. This work was supported by a Grant-in-Aid for Scientific Research (No. 06403027) from the Ministry of Education, Science, and Culture of Japan.

References and Notes

(1) Papkov, S. P.; Kulichikhin, V. G.; Kalmykova, V. D.; Malkin, A. Y. *J. Polym. Sci., Polym. Phys. Ed.* **1974**, *12*, 1753.
(2) Enomoto, H.; Einaga, Y.; Teramoto, A. *Macromolecules* **1984**, *17*, 1573.
(3) Enomoto, H.; Einaga, Y.; Teramoto, A. *Macromolecules* **1985**, *18*, 2695.
(4) Takada, Y.; Sato, T.; Teramoto, A. *Macromolecules* **1991**, *24*, 6215.
(5) Doi, M.; Edwards, S. F. *The Theory of Polymer Dynamics*; Clarendon Press: Oxford, U.K., 1986.
(6) Odijk, T. *Macromolecules* **1983**, *16*, 1340.
(7) Doi, M. *J. Polym. Sci., Polym. Symp.* **1985**, *73*, 93.
(8) Semenov, A. N. *J. Chem. Soc., Faraday Trans. 2* **1986**, *82*, 317.
(9) Sato, T.; Takada, Y.; Teramoto, A. *Macromolecules* **1991**, *24*, 6220.
(10) Sato, T.; Ohshima, A.; Teramoto, A. *Macromolecules* **1994**, *27*, 1477.
(11) Fujiyama, T.; Sato, T.; Teramoto, A. *Acta Polym.*, in press.
(12) Sato, T.; Teramoto, A. *Adv. Polym. Sci.*, in press.
(13) Itou, T.; Chikiri, H.; Teramoto, A.; Aharoni, S. M. *Polym. J.* **1988**, *20*, 143.
(14) Jinbo, Y.; Sato, T.; Teramoto, A. *Macromolecules* **1994**, *27*, 6080.
(15) Murakami, H.; Norisuye, T.; Fujita, H. *Macromolecules* **1980**, *13*, 345.
(16) Itou, T.; Teramoto, A. *Macromolecules* **1988**, *21*, 2225.
(17) Itou, T.; Sato, T.; Teramoto, A.; Aharoni, S. M. *Polym. J.* **1988**, *20*, 1049.
(18) Kuwata, M.; Murakami, H.; Norisuye, T.; Fujita, H. *Macromolecules* **1984**, *17*, 2731.
(19) Aharoni, S. M. *Macromolecules* **1979**, *12*, 94.
(20) Aharoni, S. M. *J. Polym. Sci.: Polym. Phys. Ed.* **1980**, *18*, 1439.
(21) Aharoni, S. M. *Polym. Bull.* **1981**, *5*, 95.
(22) Aharoni, S. M.; Walsh, E. K. *J. Polym. Sci., Polym. Lett. Ed.* **1979**, *17*, 321.
(23) Aharoni, S. M.; Walsh, E. K. *Macromolecules* **1979**, *12*, 271.
(24) Takada, Y.; Sato, T.; Einaga, Y.; Teramoto, A. *Bull. Inst. Chem. Res. Kyoto Univ.* **1988**, *66*, 212.
(25) Adam, M.; Delsanti, M. *J. Phys. (Paris)* **1983**, *44*, 1185.
(26) Adam, M.; Delsanti, M. *J. Phys. (Paris)* **1984**, *45*, 1513.
(27) Ferry, J. D. *Viscoelastic Properties of Polymers*, 3rd ed.; John Wiley & Sons: New York, 1980.
(28) de Gennes, P.-G. *Macromolecules* **1976**, *9*, 594.
(29) Teraoka, I.; Ookubo, N.; Hayakawa, R. *Phys. Rev. Lett.* **1985**, *55*, 2712.

MA950337Z